

Unveiling the crystalline packing of Y6 in thin films by thermal induced “backbone-on” orientation

Yiqun Xiao,^a Jun Yuan,^b Guodong Zhou,^c Ka Chak Ngan,^a Xinxin Xia,^a Jingshuai Zhu,^d Yingping Zou,^b Ni Zhao,^c Xiaowei Zhan,^d Xinhui Lu^{*a}

^aDepartment of Physics, The Chinese University of Hong Kong, Shatin, New Territories, Hong Kong, China E-mail: xinhui.lu@cuhk.edu.hk

^bCollege of Chemistry and Chemical Engineering, Central South University, Changsha 410083, P.R. China

^cDepartment of Electronic Engineering, The Chinese University of Hong Kong, Shatin, New Territories, Hong Kong, P.R. China

^dDepartment of Materials Science and Engineering, College of Engineering, Key Laboratory of Polymer Chemistry and Physics of Ministry of Education, Peking University, Beijing 100871, China

Device fabrication

Solar cells were fabricated in a conventional device configuration of ITO/PEDOT:PSS/active layer/PNDIT-F3N/Ag. The ITO substrates were first scrubbed by detergent and then sonicated

with the deionized water, acetone and isopropanol, each twice for 30 min subsequently, and finally dried with nitrogen flow. Before the spin coating, the ITO substrates were UV-Ozone treated for 20 min. PEDOT:PSS (Heraeus Clevios P VP AI 4083) was spin-coated onto the ITO substrates at 4000 rpm for 30 s, and dried at 150 °C for 10 min in the fumehood. The PM6: acceptor(s) blends (1:1.2, w/w) were dissolved in the chloroform (CF) (the total concentration of 15 mg mL⁻¹) with 1-chloronaphthalene (CN) (0.5% vol) as the additive. The solutions were stirred overnight in the glove box. The blend solutions were kept at 55°C and spin-cast at 3000 rpm for 30 s onto the PEDOT:PSS films and followed by thermal annealing treatment at 95°C for 5 min. After that, A thin layer PNDIT-F3N, was spin-coated as electron transporting layer. Finally Ag (100 nm) was thermal evaporated (<1×10⁻⁴ Pa) as the top electrodes. The optimal active layer thickness measured by a Bruker Dektak XT stylus profilometer was ~100 nm. The device area was calibrated by Optical microscope (Olympus BX3M-PSLED) as ~3.8 mm².

Electron-only devices were fabricated with the structure of ITO/ZnO/active layer/PNDIT-F3N/Ag while hole-only devices with the structure of ITO/MoO_x/active layers/MoO_x/Ag. The carrier mobilities were extracted by fitting the current density-voltage (J - V) curves using the space charge limited current (SCLC) method. The J - V curves of the devices were plotted as $\ln [Jd^3/V^2]$ versus $[V/d]^{0.5}$ using the equation

$$J = \frac{9}{8} \mu \epsilon_r \epsilon_0 \frac{V^2}{d^3} \exp \left(0.89 \left(\frac{V}{E_0 d} \right)^{0.5} \right) \quad (1)$$

where J is the current density, d is the active layer thickness (~ 100 nm), μ_h is hole mobility, μ_e is electron mobility, ϵ_r is the relative dielectric constant, and ϵ_0 is permittivity of free space (8.85 × 10⁻¹² F m⁻¹). $V = V_{\text{appl}} - V_{\text{bi}}$, V_{appl} is the applied voltage, V_{bi} is the offset voltage.

For in-plane mobility test, the field-effect transistors (FETs) were fabricated onto silicon oxide (SiO₂, 300 nm, 11.5 nF cm⁻²) covered heavily doped silicon wafer. The source/drain electrode (4

nm Cr/40 nm Au, W/L =15 × 1mm/10μm) were formed through photolithography, thermal evaporation and lift-off processes. Then the substrate was cleaned, went through gas self-assembled monolayer (SAM) treatment, and was post-cleaned as in ref¹ for organic FETs. Afterwards the active layer of three material systems was spin-coated at 3000 rpm to keep the film thickness of ~100nm and annealed at 100°C for 10 min in nitrogen glovebox.

Characterization

Device Characterization.

The J - V curves of all encapsulated devices were measured using a Keithley 2612 Source Meter in air under AM 1.5G (100 mW cm⁻²) with a Newport solar simulator. The light intensity was calibrated using a standard Si diode. EQE spectra were measured using an Enlitech QE-S EQE system equipped with a standard Si solar cell calibration. Monochromatic light was generated from a Newport 300W Xeon lamp source. UV-Vis absorption spectra were taken on a Cary 5G UV-Vis-NIR spectrophotometer.

Mobility Measurements.

The transfer characteristics of FETs was measured by Keithley 2612B dual-channel source meter in nitrogen glovebox in dark condition. The gate voltage V_{gs} was scanned from 50 V to -50 V with the source-drain voltage V_{ds} set at -60V, the source-drain and gate leakage current was recorded during the scanning. The in-plane mobility was extracted in saturation regime with:

$$\mu = \frac{2L}{C_i W} \left(\frac{\partial \sqrt{|I_{ds}|}}{\partial V_{gs}} \right)^2$$
. Linear $\sqrt{|I_{ds}|} - V_{gs}$ fitting ranges were chosen to extract the hole and electron mobilities.

Morphology Characterization.

The grazing incidence wide angle/small angle X-ray scattering (GIWAXS/SAXS) measurement

was carried out with a Xeuss 2.0 SAXS/WAXS laboratory beamline using a Cu X-ray source (8.05 keV, 1.54 Å) and a Pilatus3R 300K detector. The incident angle was 0.2°. The samples for GIWAXS/GISAXS measurement were fabricated on the silicon substrates using the same recipe for the devices. Then the films were thermal annealed at the set temperatures for 5 minutes.

Thermogravimetric Analysis (TGA).

TGA was measured on PerkinElmer TGA6 Thermogravimetric Analyzer. The temperature rising rate was 10 ° C min⁻¹ in the nitrogen atmosphere.

Differential Scanning Calorimetry (DSC).

DSC measurement was measured on PerkinElmer PYRIS1 Differential Scanning Calorimeter. We took 2 circles of measurement, both the first and second circles are starting from 50 to 310 ° C/410 ° C then back to 50 ° C. The heating/cooling rate was 10 ° C min⁻¹ in nitrogen atmosphere.

Surface Tension Characterization.

Contact angle measurements were carried out by an Attension Theta Flex meter, using water and ethylene glycol by sessile drop analysis. The surface tension values of films are calculated by Fowkes approximation,² where $(\cos \theta + 1)^2 = 4 \gamma_{sd} \gamma_{ld} / \gamma_L^2$, where γ_{sd} and γ_{ld} refer to dispersion tension of plane surface and liquid, while γ_L refers to total tension of liquid.

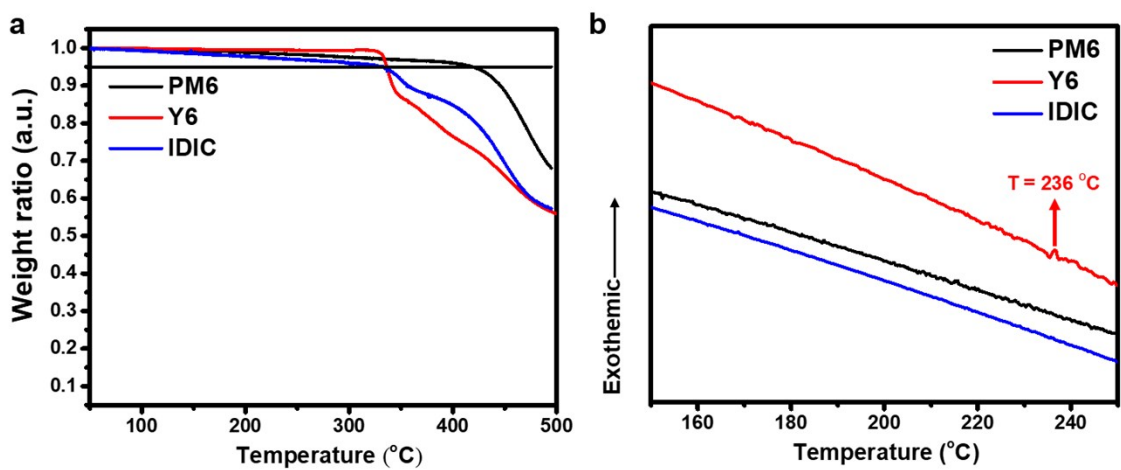


Figure S1. (a) TGA and (b) DSC curves for PM6, Y6, IDIC. The decomposition temperature of materials obtained from TGA data is the 5% weight loss temperature.

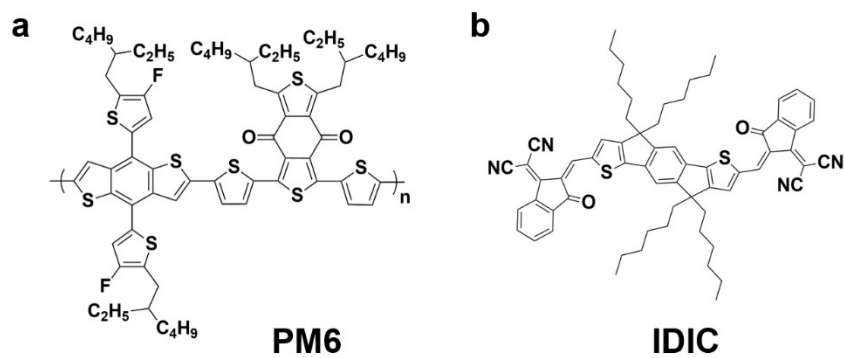


Figure S2. Chemical structures of (a) PM6 and (b) IDIC.

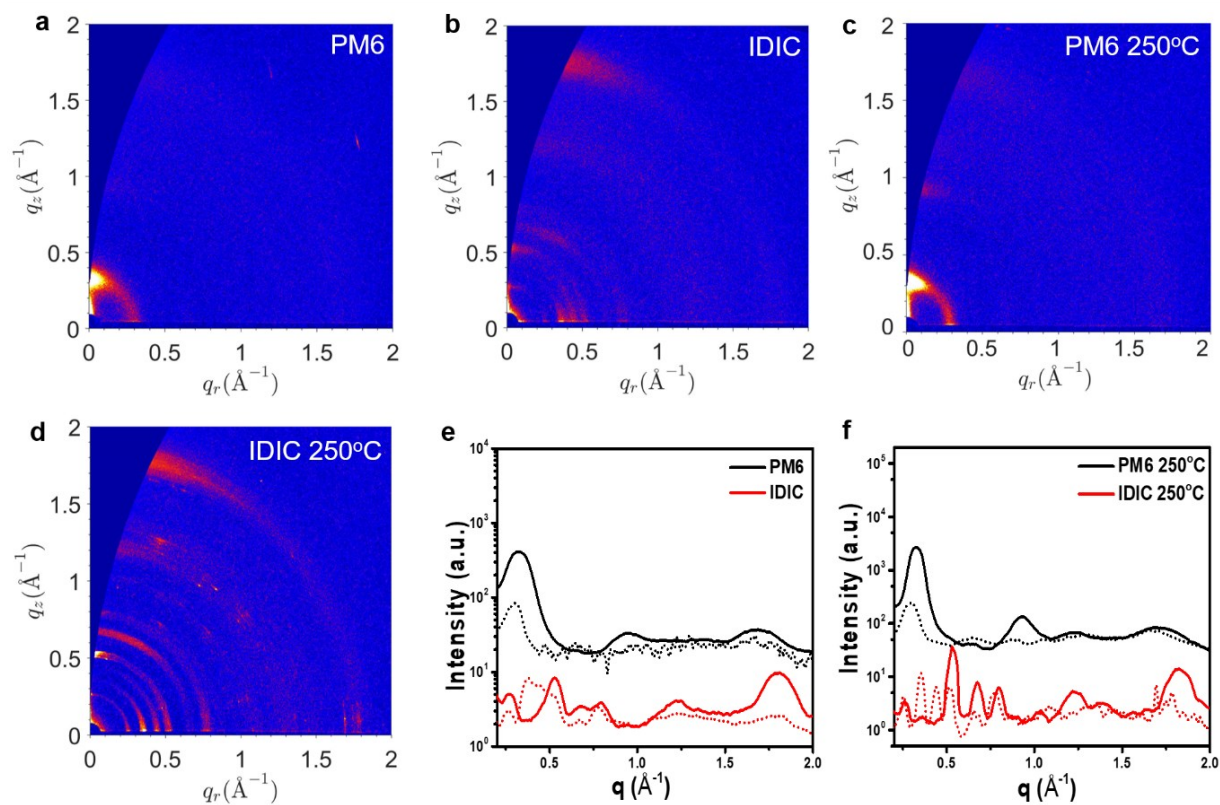


Figure S3. 2D GIWAXS pattern of pure PM6 annealed at (a) 95°C (optimized device temperature) and (b) 250°C, and IDIC films at (c) 95°C and (d) 250°C; the corresponding line-cuts along in-plane (IP) (dashed lines) and out-of-plane (OOP) (solid lines) directions of films annealed at (e) 95°C and (f) 250°C.

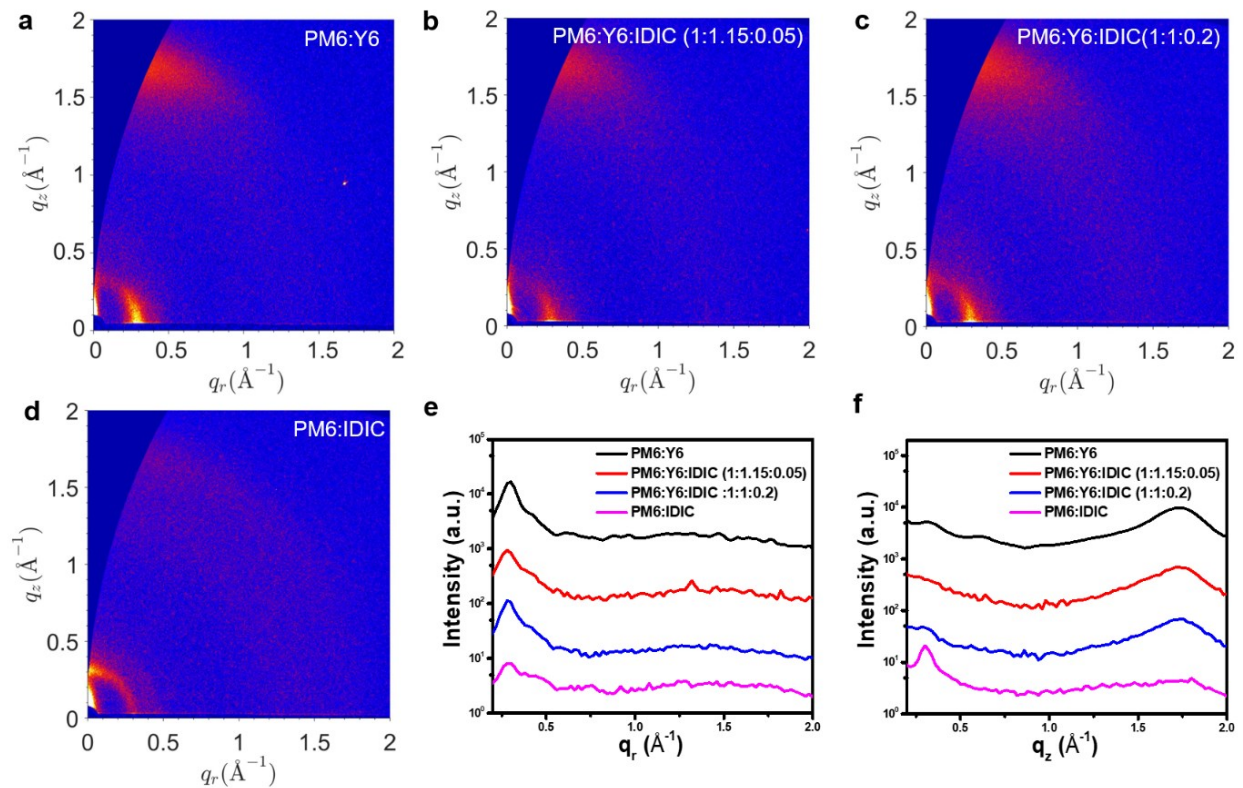


Figure S4. 2D GIWAXS pattern of (a) PM6:Y6, (b) PM6:Y6:IDIC (1:1.15:0.05), (c) PM6:Y6:IDIC (1:1:0.2) and (d) PM6:IDIC blend films annealed at 95°C; the corresponding intensity profiles along (e) IP and (f) OOP directions.

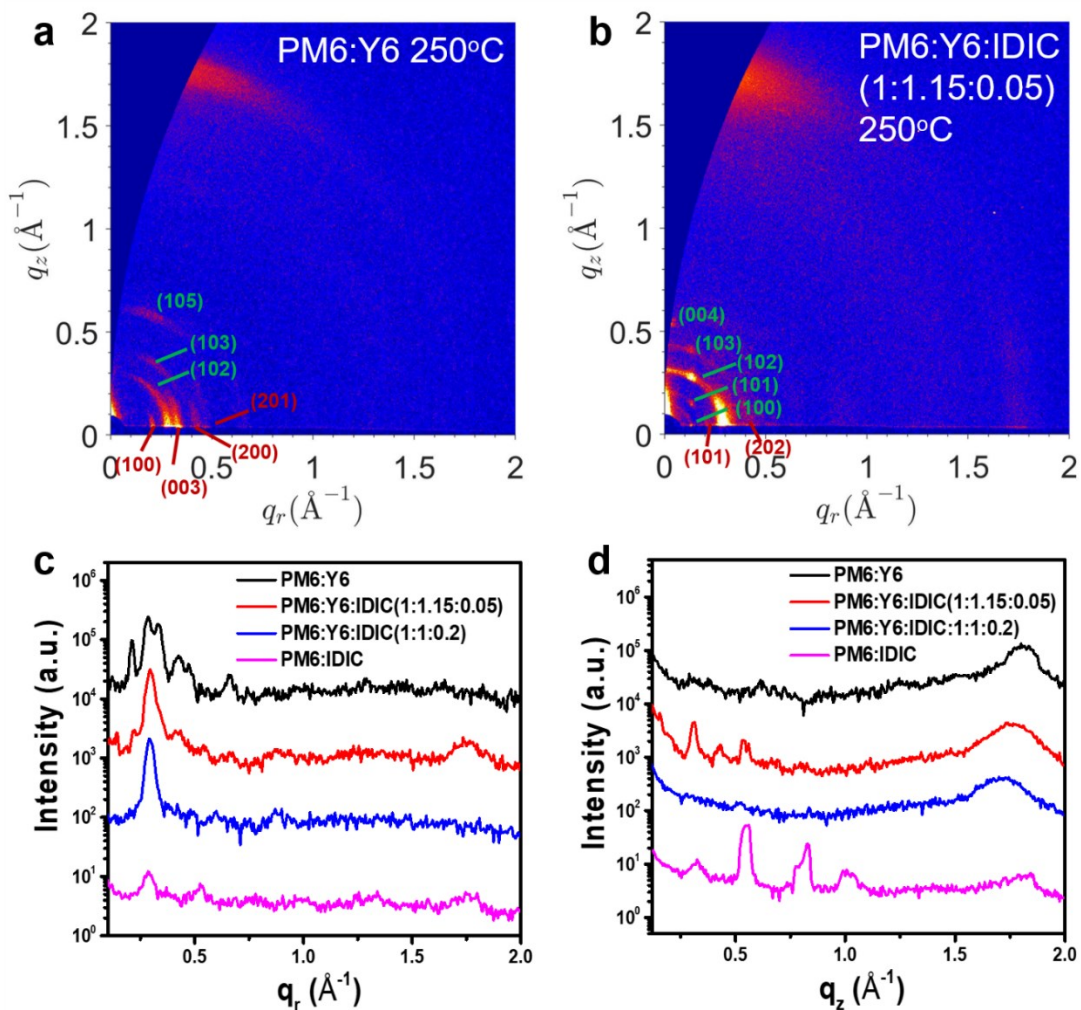


Figure S5. GIWAXS pattern of (a) binary PM6:Y6 and (b) ternary PM6:Y6:IDIC (1:1.15:0.05) blend films with peak indexed (red/green indices for backbone-on/face-on orientation) and the intensity profiles along (c) IP and (d) OOP directions of all binary and ternary blend films annealed at 250°C.

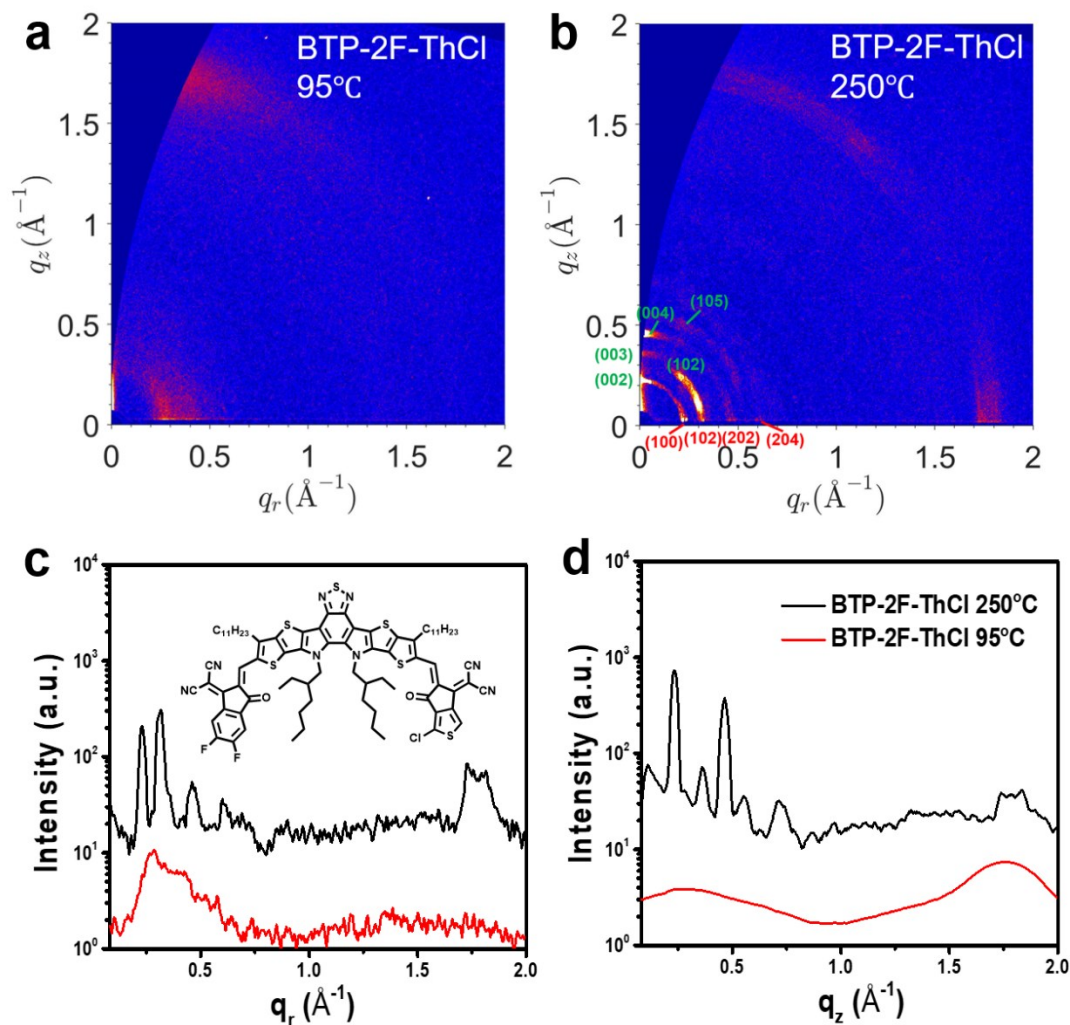


Figure S6. GIWAXS pattern of pure BTP-2F-ThCl film annealed at (a) 95 °C and (b) 250°C (peak indices: red/green indices for backbone-on/face-on orientation); the intensity profiles along (c) IP (inset: chemical structure of BTP-2F-ThCl) and (d) OOP directions of all binary and ternary blend films annealed at 250°C.

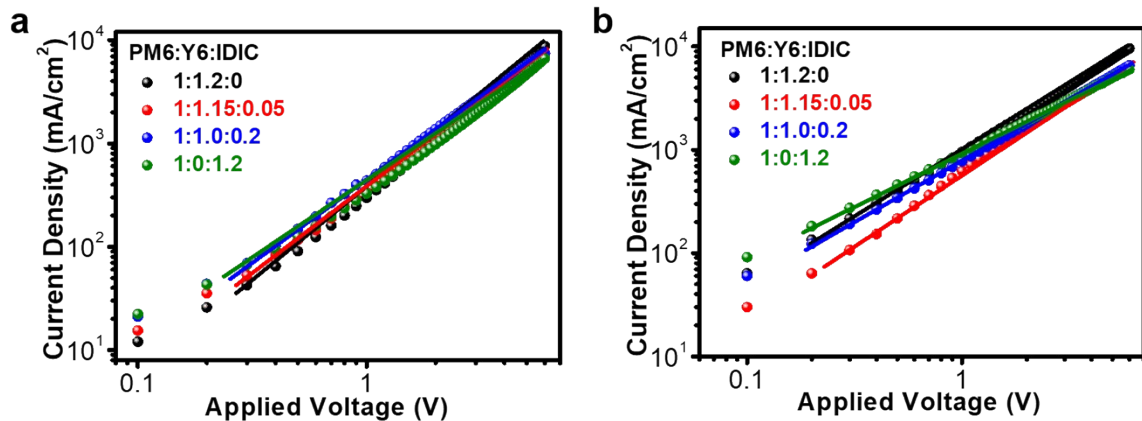


Figure S7. (a) J - V characteristics in the dark for (a) hole-only and (b) electron-only devices based on binary and ternary blend films.

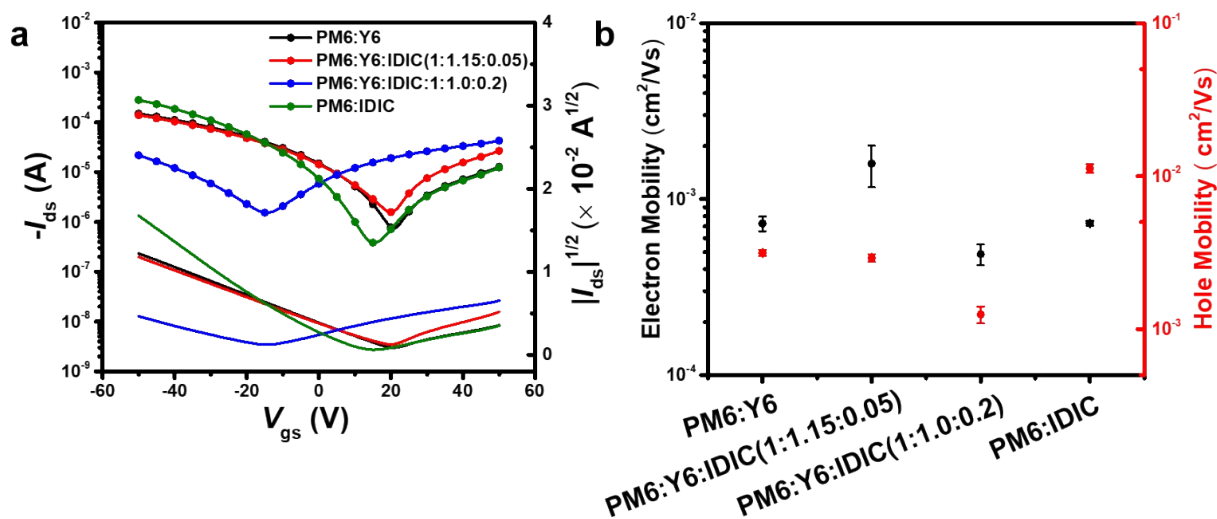


Figure S8. (a) Transfer characteristics in the saturation region ($V_{ds} = -60$ V) of bottom-gated FET devices in the dark; (b) extracted in-plane hole and electron mobilities of the binary and ternary blend films.

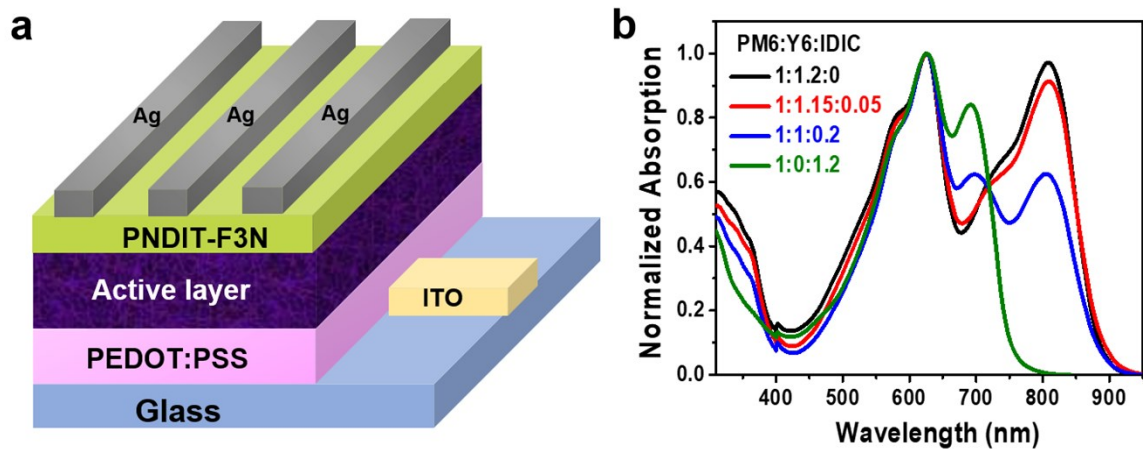


Figure S9. (a) Conventional device structure of the OSCs; (b) UV-vis light absorption spectra of the blend films.

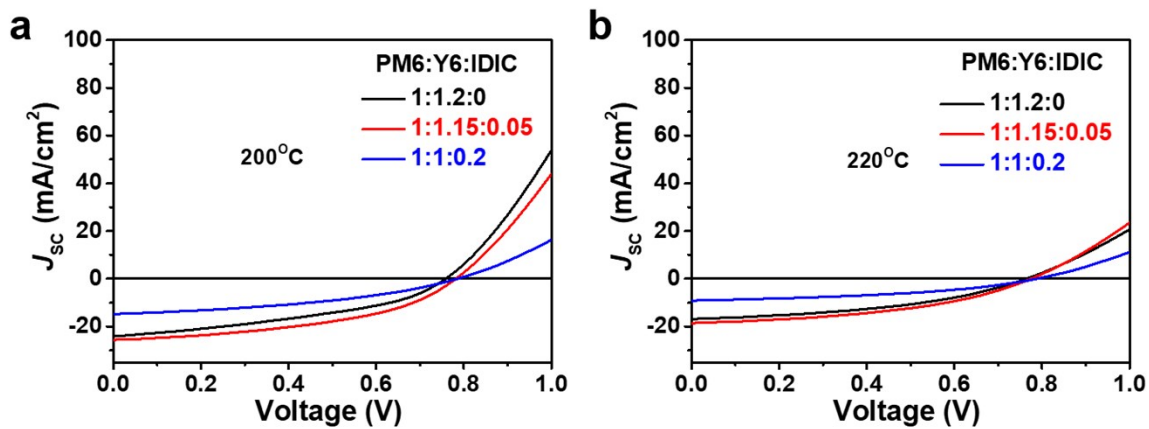


Figure S10. J - V curves of binary and ternary Y6 based devices with different mass ratios annealed at (a) 200°C and (b) 220°C.

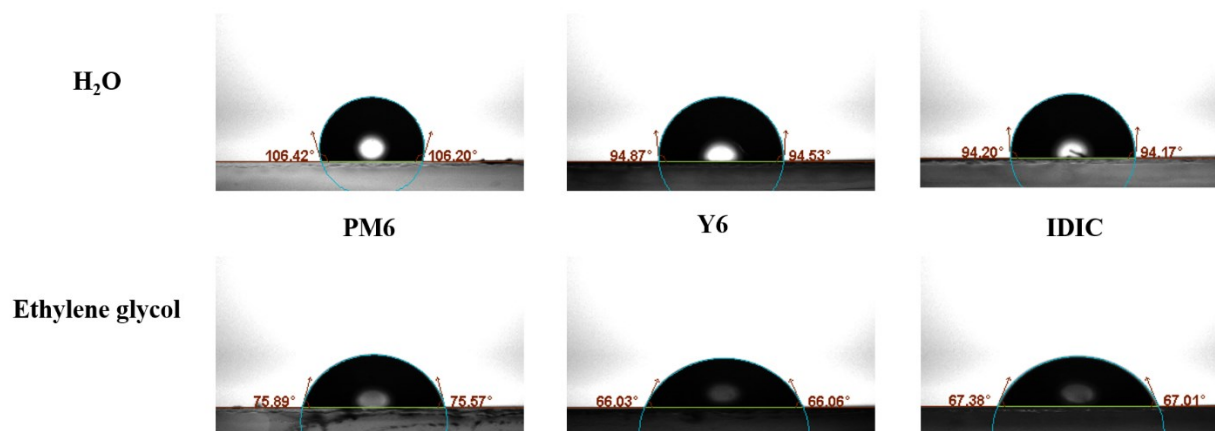


Figure S11. Contact angle images of pure PM6, Y6, and IDIC films with water and ethylene glycol droplet on the top surface.

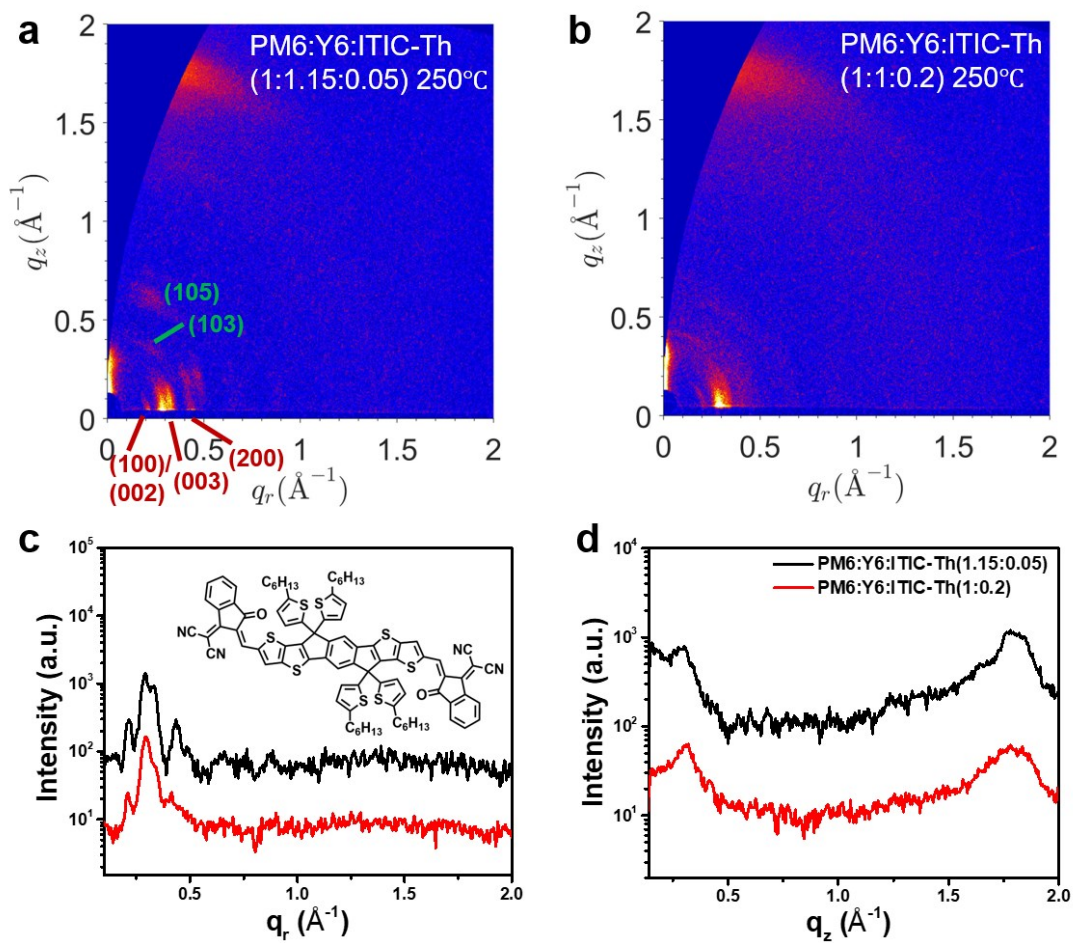


Figure S12. 2D GIWAXS patterns of (a) PM6:Y6:ITIC-Th (1:1.15:0.05) and (b) PM6:Y6:ITIC-Th (1:1:0.2) films (peak indexed with rectangle lattice constants, the red indices for face-on orientation while green indices for backbone on orientation); the corresponding intensity profiles along (c) in-plane (inset: chemical structure of ITIC-Th) and (d) out-of-plane directions.

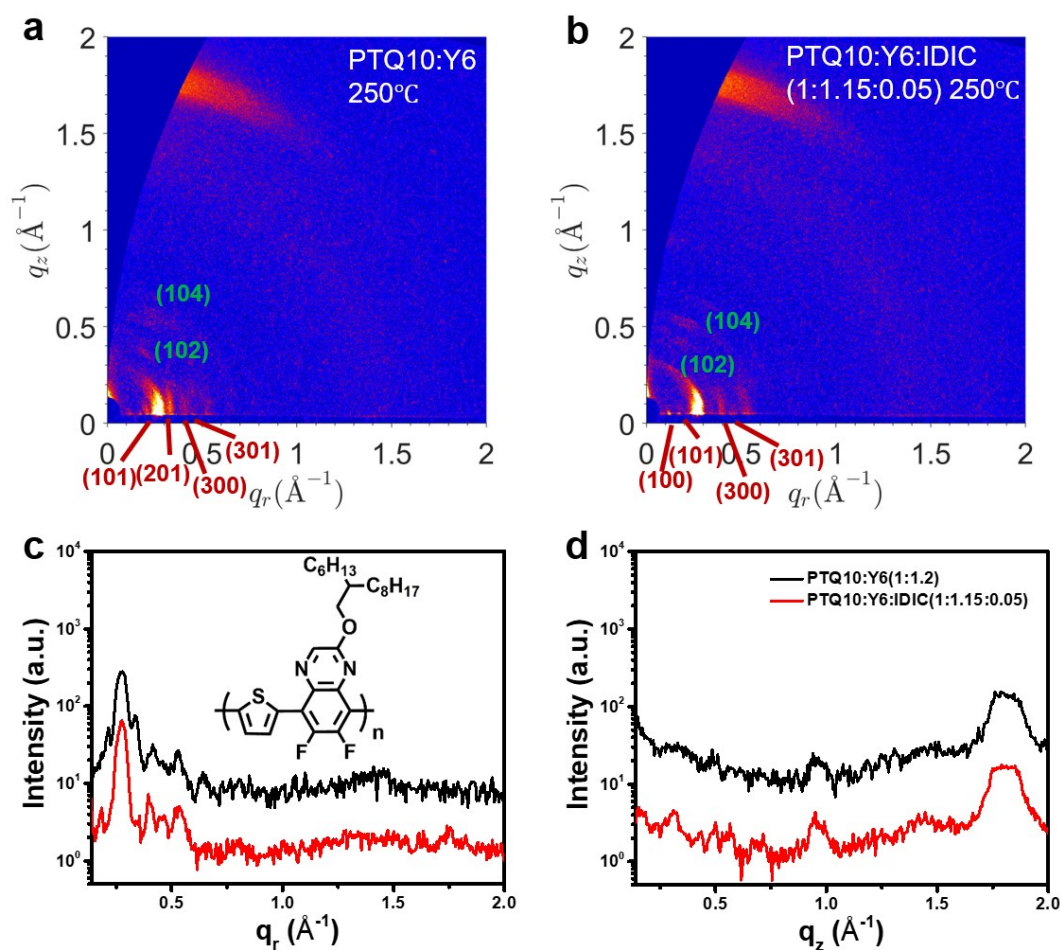


Figure S13. 2D GIWAXS patterns of (a) PTQ10:Y6 and PTQ10:Y6:IDIC (1:1.15:0.05) films (peak indexed with square lattice constants, the red indices for face-on orientation while green indices for backbone on orientation) annealed at 250°C; the corresponding intensity profiles along (c) in-plane (inset: chemical structure of PTQ10) and (d) out-of-plane directions.

Table S1. Electron mobilities in the IP and the OOP direction extracted via FET and SCLC methods.

PM6:Y6:IDIC	IP μ_e via FET method ($\text{cm}^2 \text{V}^{-1} \text{s}^{-1}$)	OOP μ_e via SCLC method ($\text{cm}^2 \text{V}^{-1} \text{s}^{-1}$)
1:1.2:0	7.60×10^{-4}	4.67×10^{-4}
1:1.15:0.05	1.49×10^{-3}	4.80×10^{-4}
1:1.0:0.2	5.85×10^{-4}	3.88×10^{-4}
1:0:1.2	7.10×10^{-4}	3.74×10^{-4}

Table S2. Hole mobilities in the IP and the OOP direction extracted via FET and SCLC methods.

PM6:Y6:IDIC	In-plane μ_h via FET method ($\text{cm}^2 \text{V}^{-1} \text{s}^{-1}$)	Out-of-plane μ_h via SCLC method ($\text{cm}^2 \text{V}^{-1} \text{s}^{-1}$)
1:1.2:0	3.27×10^{-3}	7.81×10^{-4}
1:1.15:0.05	2.97×10^{-3}	7.69×10^{-4}
1:1.0:0.2	1.38×10^{-3}	7.55×10^{-4}
1:0:1.2	10.2×10^{-3}	7.44×10^{-4}

Table S3. Device performance of the binary and ternary Y6 based OSCs annealed at 200°C.

PM6:Y6:IDIC	V_{oc} (V)	J_{sc} (mA cm^{-2})	FF (%)	PCE (%)
1:1.2:0	0.759 (0.757±0.006)	24.15 (23.20±0.82)	40.2 (38.9±0.8)	7.13 (6.84±0.39)
1:1.15:0.05	0.781 (0.778±0.012)	25.56 (25.50±0.14)	45.0 (44.2±1.0)	8.99 (8.76±0.31)
1:1:0.2	0.785 (0.788±0.003)	14.83 (14.25±0.68)	39.1 (38.9±0.7)	4.56 (4.37±0.28)

The data in bracket are averaged over 5 devices.

Table S4. Device performance of the binary and ternary Y6 based OSCs annealed at 220°C.

PM6:Y6:IDIC	V_{oc} (V)	J_{sc} (mA cm ⁻²)	FF (%)	PCE (%)
1:1.2:0	0.763 (0.767±0.006)	16.99 (16.90±0.10)	42.5 (42.0±0.5)	5.51 (5.45±0.08)
1:1.15:0.05	0.781 (0.780±0.005)	16.90 (17.19±1.22)	45.0 (42.2±0.6)	6.16 (5.66±0.44)
1:1:0.2	0.788 (0.785±0.005)	9.18 (8.93±0.22)	41.3 (40.8±0.7)	2.99 (2.86±0.28)

The data in bracket are averaged over 5 devices.

Table S5. Calculated results from J_{ph} - V_{eff} curves.

PM6:Y6:IDIC	J_{sat}^c	J_{ph}^{ac}	J_{ph}^{bc}	J_{ph}^{ac} / J_{sat}^c	J_{ph}^{bc} / J_{sat}^c
1:1.2:0	27.460	25.493	22.803	92.8%	83.0%
1:1.15:0.05	27.315	25.671	23.100	94.0%	84.6%
1:0:1.2	16.879	15.641	13.436	92.7%	79.6%

J_{ph} values under (a) short-circuit and (b) maximal output condition.

(c) The unit is mA cm⁻².

Table S6. Morphology parameters (ξ is the intermixing domain size; $2R_{g-fractal}$ is the acceptor domain size) fitted by GISAXS profiles of the blend films.

PM6:Y6:IDIC	ξ (nm)	$2R_{g-fractal}$ (nm)
1:1.2:0	49	17
1:1.15:0.05	38	22
1:1.0:0.2	47	24
1:0:1.2	69	20

Table S7. Contact Angles and Surface Tensions (γ).

Surface	$\theta_{\text{water}}(^{\circ})$	$\theta_{\text{EG}}(^{\circ})$	γ (mN m^{-1}) ^a	χ^{b}
PM6	106.31	75.73	27.88	$\chi^{\text{PM6,Y6}}=0.017$
Y6	94.70	66.04	26.54	$\chi^{\text{Y6,IDIC}}=0.007$
IDIC	94.19	67.19	25.66	$\chi^{\text{PM6,IDIC}}=0.046$

Surface Free Energy is calculated via Wu method.

^a The Flory–Huggins interaction parameters based on the surface tension data formula.²

^b The Flory–Huggins interaction parameters between material A and material B are calculated using

$$\chi^{\text{A,B}} = (\sqrt{\gamma^{\text{A}}} - \sqrt{\gamma^{\text{B}}})^2.$$

References

1. G. D. Zhou, S. Zhou, Q. Zhu and N. Zhao, *Adv. Electron. Mater.*, 2019, **5**, 1900055.
2. F. M. Fowkes, *Ind. Eng. Chem.*, 1964, **56**, 40-52.